Prognostic Value of Multiplexed Assays of Variant Effect and Automated Patch-clamping for *KCNH2*-LQTS Risk Stratification

Matthew J. O'Neill[1,17], Chai-Ann Ng[2,3,17], Takanori Aizawa[4], Luca Sala[5], Sahej Bains[6], Isabelle Denjoy[7], Annika Winbo[8], Rizwan Ullah[9], Qianyi Shen[2], Chek-Ying Tan[2], Krystian Kozek[9], Loren R. Vanags[9], Devyn W. Mitchell[9], Alex Shen[9], Yuko Wada[9], Asami Kashiwa[4], Lia Crotti[5,10], Federica Dagradi[5], Giulia Musu[5], Carla Spazzolini[5], Raquel Neves[6], J. Martijn Bos[6], John R. Giudicessi[6], Xavier Bledsoe[1], Megan Lancaster[9], Andrew M. Glazer[9], Dan M. Roden[9], Antoine Leenhardt[7], Joe-Elie Salem[7], Nikki Earle[11], Rachael Stiles[12], Taylor Agee[13], Christopher N. Johnson[13], Minoru Horie[14], Jonathan Skinner[15], Fabrice Extramiana[7], Michael J. Ackerman[6], Peter J. Schwartz[5], Seiko Ohno[16], Jamie I. Vandenberg*[2,3], Brett M. Kroncke*[9]

1. Vanderbilt University School of Medicine, Medical Scientist Training Program, Nashville, TN, USA
2. Mark Cowley Lidwill Research Program in Cardiac Electrophysiology, Victor Chang Cardiac Research Institute, Darlinghurst, NSW, Australia
3. School of Clinical Medicine, UNSW Sydney, Darlinghurst, NSW, Australia
4. Department of Cardiovascular Medicine, Kyoto University Graduate School of Medicine Kyoto, Japan
5. IRCCS, Istituto Auxologico Italiano, Center for Cardiac Arrhythmias of Genetic Origin and Laboratory of Cardiovascular Genetics, Milano, Italy
6. Department of Molecular Pharmacology & Experimental Therapeutics (Windland Smith Rice Sudden Death Genomics Laboratory), Mayo Clinic, Rochester, MN, USA
7. Department of Cardiovascular Medicine, Hôpital Bichat, APHP, Université de Paris Cité, Paris, France
8. Department of Physiology, University of Auckland, Auckland, New Zealand
9. Vanderbilt Center for Arrhythmia Research and Therapeutics, Division of Clinical Pharmacology, Department of Medicine, Vanderbilt University Medical Center, Nashville, TN, USA
10. Department of Medicine and Surgery, University Milano Bicocca, Milan, Italy
11. Department of Medicine, University of Auckland, Auckland, New Zealand
12. Department of Cardiology, Waikato Hospital, Hamilton, New Zealand
13. Department of Chemistry, Mississippi State University, Starkville, MS 39759, USA
14. Department of Cardiovascular Medicine, Shiga University of Medical Science, Shiga, Japan
15. Sydney Children's Hospital Network, University of Sydney, Sydney, Australia
16. Department of Bioscience and Genetics, National Cerebral and Cardiovascular Center, Osaka, Japan
17. These authors contributed equally

*Correspondence to

Jamie I. Vandenberg, MBBS, Ph.D., Victor Chang Cardiac Research Institute, 405 Liverpool St, Darlinghurst, NSW 2010, Australia. E-mail: j.vandenberg@victorchang.edu.au; Tel: +61 2 9295 8687

and

Brett M. Kroncke, Ph.D., Vanderbilt University Medical Center, Office 1215E Light Hall/Medical Research Building IV, 2215 Garland Avenue, Nashville, TN, USA 37232. Email: brett.m.kroncke.1@vumc.org; Tel: +1-608-658-8372

Abstract

Background: Long QT syndrome (LQTS) is a lethal arrhythmia condition, frequently caused by rare loss-of-function variants in the cardiac potassium channel encoded by *KCNH2*. Variant-based risk stratification is complicated by heterogenous clinical data, incomplete penetrance, and low-throughput functional data.
Objective: To test the utility of variant-specific features, including high-throughput functional data, to predict cardiac events among *KCNH2* variant heterozygotes.
Methods: We quantified cell-surface trafficking of 18,323 variants in *KCNH2* and recorded potassium current densities for 506 *KCNH2* variants. Next, we deeply phenotyped 1150 *KCNH2* missense variant patients, including ECG features, cardiac event history (528 total cardiac events), and mortality. We then assessed variant functional, *in silico*, structural, and LQTS penetrance data to stratify event-free survival for cardiac events in the study cohort.
Results: Variant-specific current density (HR 0.28 [0.13-0.60]) and estimates of LQTS penetrance incorporating MAVE data (HR 3.16 [1.59-6.27]) were independently predictive of severe cardiac events when controlling for patient-specific features. Risk prediction models incorporating these data significantly improved prediction of 20 year cardiac events (AUC 0.79 [0.75-0.82]) over patient-only covariates (QTc and sex) (AUC 0.73 [0.70-0.77]).
Conclusion: We show that high-throughput functional data, and other variant-specific features, meaningfully contribute to both diagnosis and prognosis of a clinically actionable monogenic disease.

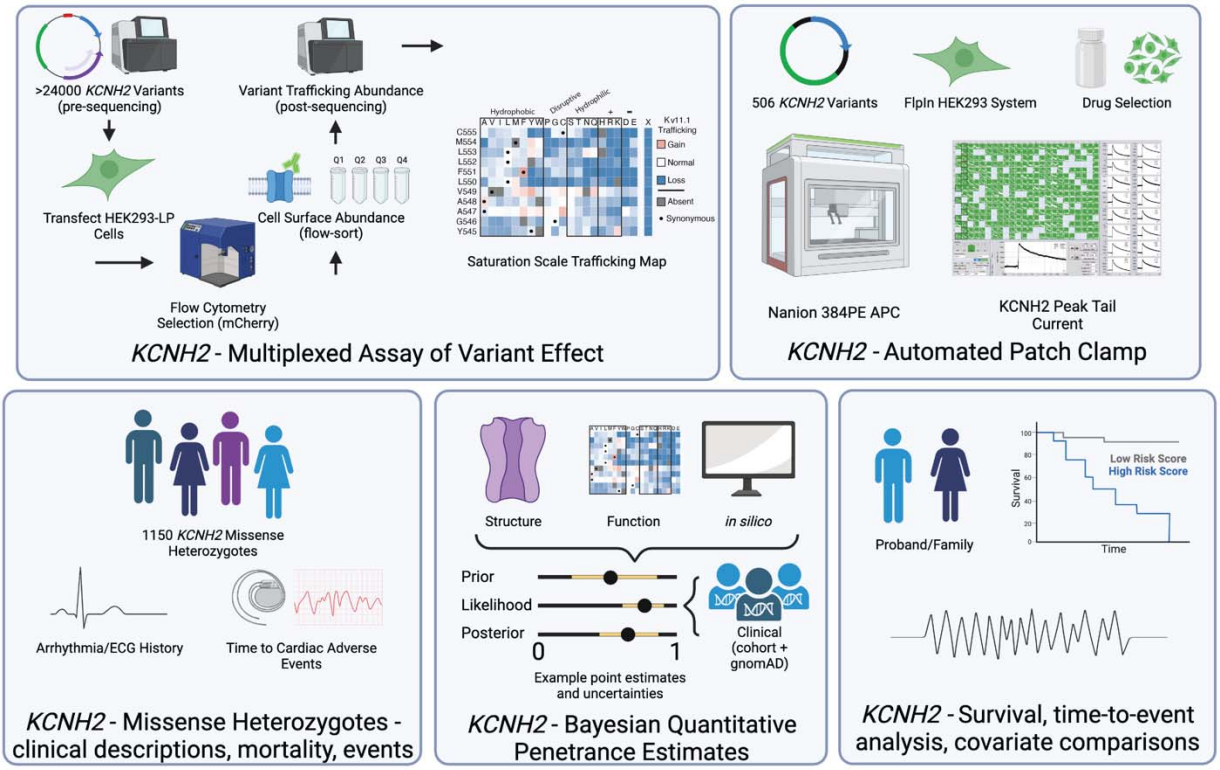

Graphical Abstract. Implementation of *KCNH2* variant functional studies, deep clinical phenotyping, and cardiac event risk stratification.

Main Text

Congenital Long QT Syndrome (LQTS) is a frequently fatal inherited arrhythmia syndrome with strong monogenic contributions[1]. Rare, loss-of-function variants in *KCNH2*, which encodes for the cardiac repolarizing potassium ion channel current I_{Kr}, are implicated in approximately 30% of Long QT syndrome cases (LQT2)[2]. Integrating genetic data into clinical practice is hindered by complex variant interpretation, incomplete penetrance, and environmental interactions. Variant-specific information, including functional data, can assist with variant classification and diagnosis[3,4]; however, whether variant-specific information can assist with prognosis is unknown. Here, we implemented two high-throughput functional assays to study the *KCNH2*-LQT2 relationship: 1) Multiplexed Assays of Variant Effect (MAVE)[5,6], and 2) Automated Patch Clamping (APC)[7]. The MAVE probed the effect on protein trafficking of nearly all possible *KCNH2* missense variants, providing prospective evidence for unascertained variant future classification[8]. APC recorded detailed effects on variant protein electrophysiological function after clinical ascertainment. To evaluate the significance of these and other variant-specific attributes in stratifying the risk of LQTS events, we recorded QTc, survival data, and cardiac events in 1150 patients heterozygous for *KCNH2* missense or in-frame insertion/deletion variants.

We quantified the trafficking effect of 18,323 total variants by MAVE (Figure 1A; Supplemental Table 1)[5,6,9]. We observed excellent stratification of WT normalized variant trafficking scores across synonymous (mean 100.4±23.9%), missense (mean 71.4±46.4%), and nonsense (mean 17.9±36.0%) variant classes (Figure 1B/C; Supplemental Table 2). Consistent with a previous study, nonsense variation had minimal effect on trafficking function downstream of residue 863 (Supplemental Figure 1)[10]. In parallel, we used the SyncroPatch 384 PE platform to comprehensively interrogate potassium peak tail currents among *KCNH2* variants observed in our clinical cohorts, the literature, and gnomAD[11] (Figure 1D; Supplemental Methods). 266/506 variants had severe loss of function ($Z < -4$, Figure 1E, Supplemental Table 3) with good concordance between MAVE and APC datasets, including across “hot spot domains” (Figure 1F-G; Supplemental Figure 2). We derived ClinGen-recommended assay calibration and Z-score thresholds using the same set of variant controls for the MAVE dataset as our previously described *KCNH2* APC assay[12,13] (Supplemental Figure 3 and Supplemental Table 4). This calibration showed that the MAVE data may prospectively apply strong pathogenic functional criteria and moderate benign functional criteria. Most variants studied in both assays were concordantly annotated with an abnormal threshold of an assay Z-score less than -2 (365/420; Figures 1F and Supplemental Figure 4). 23 variants had normal trafficking but abnormal current density, suggesting abnormalities in gating or ion permeability.

We next collected clinical data on 1150 patients recruited from five tertiary arrhythmia clinics in Japan (N=289), Italy (N=275), the USA (N=261), France (N=259), and New Zealand (N=66) heterozygous for 317 unique *KCNH2* missense or in-frame insertion/deletion variants. LQTS was diagnosed based on Schwartz score >3.5 or repeated Corrected QT intervals (QTc) >480 ms without secondary causes (see methods for full details)[14]. Events were either ventricular tachycardia, ventricular fibrillation, sudden cardiac death, appropriate ICD shocks, and/or syncope; severe

events did not include syncope unless while on beta blockers. QTc intervals were higher among probands than family members (N = 503/1150; mean 504±55 vs 472±69 ms, respectively; Figure 2A), females than males (N = 606/1150; mean 494±52 vs 477±77 ms; Figure 2B), and individuals experiencing cardiac events (N = 323/1150, mean 515±59 vs 474±64 ms, respectively; Figure 2C).

Clinical risk stratification of LQTS-cardiac events currently relies on patient-specific features such as sex and QTc[15]. We hypothesized that including variant-specific data (e.g., variant functional, *in silico*, and structural properties) alongside patient-specific data could improve prognosis of adverse events. In a risk model using patient-specific QTc and sex, both functional datasets were significantly associated with event risk (Figure 2D-E). We integrated prospectively available MAVE data from the current study into our previously described Bayesian prospective LQTS penetrance tool (referenced here as 'Penetrance'; data hosted at variantbrowser.org for community use)[16]. Among 1117 patients with sex, QTc, and a LQTS penetrance estimate, we observed 296 cardiac events through the age of 40. To build a more comprehensive model, we tested the inclusion of additional variant predictive features. We reduced model complexity to the most significant covariates using multiple approaches detailed in the Supplemental Methods and Supplemental Figures 5-7. Using a Royston-Parmar time-to-event model, we observed optimal prognostic value incorporating MAVE functional into our LQTS penetrance prediction feature (Figure 2F)[17,18]. Interestingly, we observed in Figure 2F that MAVE data not integrated into this model became significantly protective when both APC and MAVE were included in the same model. This may be explained by greater phenotype resiliency against disrupted trafficking versus disrupted gating (consistent with possible dominant negative vs haploinsufficiency mechanisms)[19]. These findings show that prospectively available MAVE data provide near equivalent functional evidence strength for variant classification (diagnosis); however, APC data collected after variant ascertainment can provide additional data for event risk stratification (prognosis).

We next built a risk stratification model combining the significant predictors and demonstrated excellent performance in stratifying event risk (Figure 2G). We then compared model accuracy using an ROC/AUC approach (Figure 2H and 2I). We found that prospective (patient-specific features + LQTS penetrance estimate conditioned by MAVE data) and a model including prospective and APC data both significantly improved upon prognosis from patient-specific features alone. Lastly, we provide sex-stratified nomograms of our risk prediction model of events at 20 years for variants with prospectively available LQTS penetrance estimate (Supplemental Figure 8).

We present the first comprehensive high-throughput functional studies of a ClinGen definitive evidence LQTS-associated gene[2]. We demonstrate that integrating continuous and quantitative, variant-specific features with detailed clinical phenotyping improves risk assessment for a 'monogenic' genotype-phenotype relationship. We propose that similar approaches involving continuous variant-specific features, such as high-throughput functional studies and quantitative penetrance estimates, will further improve risk stratification in other gene-disease pairs.

Online Methods

Full methods are described in the online appendix. All clinical data used in this analysis received IRB/REC approval. The research reported in this paper adhered to guidelines included in the Helsinki Declaration as revised in 2013. All code used to analyze these data may be found on GitHub at https://github.com/kroncke-lab.

Funding

This research was funded by the National Institutes of Health: F30HL163923-01 (MJO), T32GM007347 (MJO), R01HL164675 (AMG, DMR, and BMK), and R01HL160863 (BMK); by the Leducq Transatlantic Network of Excellence Program 18CVD05 (LS, LC, PJS, and BMK); by the New South Wales Cardiovascular Disease Senior Scientist grant (JIV), and a Medical Research Future Fund: Genomics Health Futures Mission grant MRF2016760 (CAN/JIV). Flow cytometry experiments were performed in the Vanderbilt Flow Cytometry Shared Resource. The Vanderbilt Flow Cytometry Shared Resource is supported by the Vanderbilt Ingram Cancer Center (P30 CA68485) and the Vanderbilt Digestive Disease Research Center (DK058404). We also acknowledge support from the Victor Chang Cardiac Research Institute Innovation Centre, funded by the NSW Government

Data and Code Availability

Code used to analyze raw data and generate figures and tables are available at the Kroncke Lab GitHub site. Bayesian variant functional scores for MAVE and APC, *in silico* predictions, structural features, and clinical data are available at variantbrowser.org. Participant-level data are not included for concern of reidentification and privacy protection.

Acknowledgements

We thank Kenneth Matreyek and Doug Fowler for the HEK293 landing pad cells. Figures were made using BioRender.

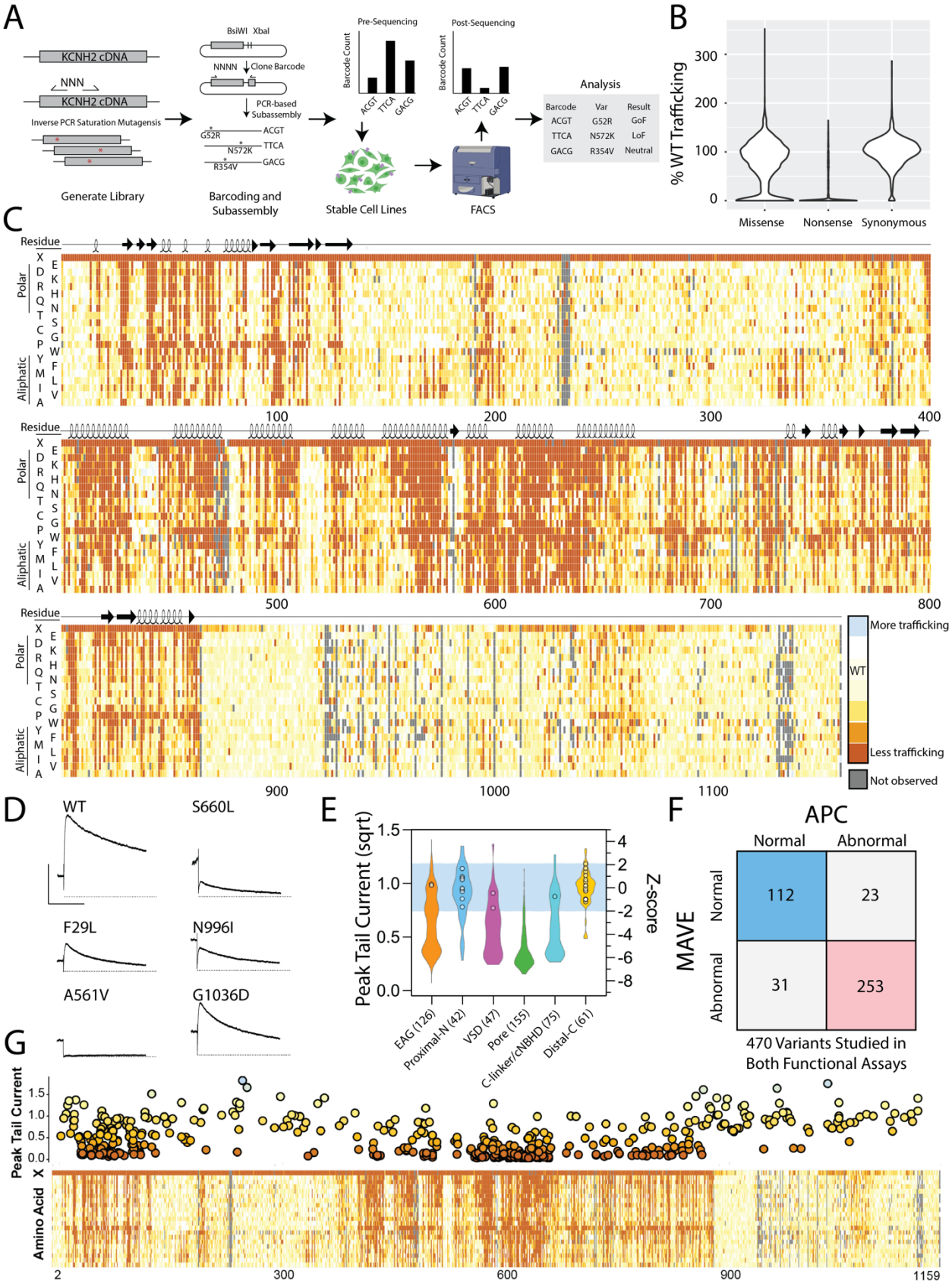

Figure 1. Implementation of *KCNH2* MAVE and APC Assays.

A) Schematic of MAVE assay. We employed a barcode abundance-based MAVE of cell-surface *KCNH2* variant expression to quantify variant trafficking, the primary mechanism of *KCNH2* variant loss-of-function.

B) Distribution of WT-normalized variant trafficking scores among missense, synonymous, and nonsense variants.

C) Heatmap depicting trafficking scores across the coding region of *KCNH2*. Dark orange indicated less than WT trafficking, white similar trafficking to WT, and blue increased trafficking. Missing data are depicted in gray.

D) Example APC peak tail currents recorded at -50 mV showing different levels of function. Y-axis is 500 pA and X-axis is 500ms.

E) KCNH2 peak-tail current densities for 506 variants (n=36,565 recordings) across 6 domains of the protein observed in our clinical cohort, gnomAD[11], and previous literature reports[20]. Benign variant controls from gnomAD are shown as white circles. Blue range depicts variants with 'normal function', as defined by a ±2 Z-score window from the mean current density for B/LB variants[12].

F) Matrix of Z-score determined normal and abnormal variants studied by both functional assays.

G) Visual correlation of functional assays by residue position.

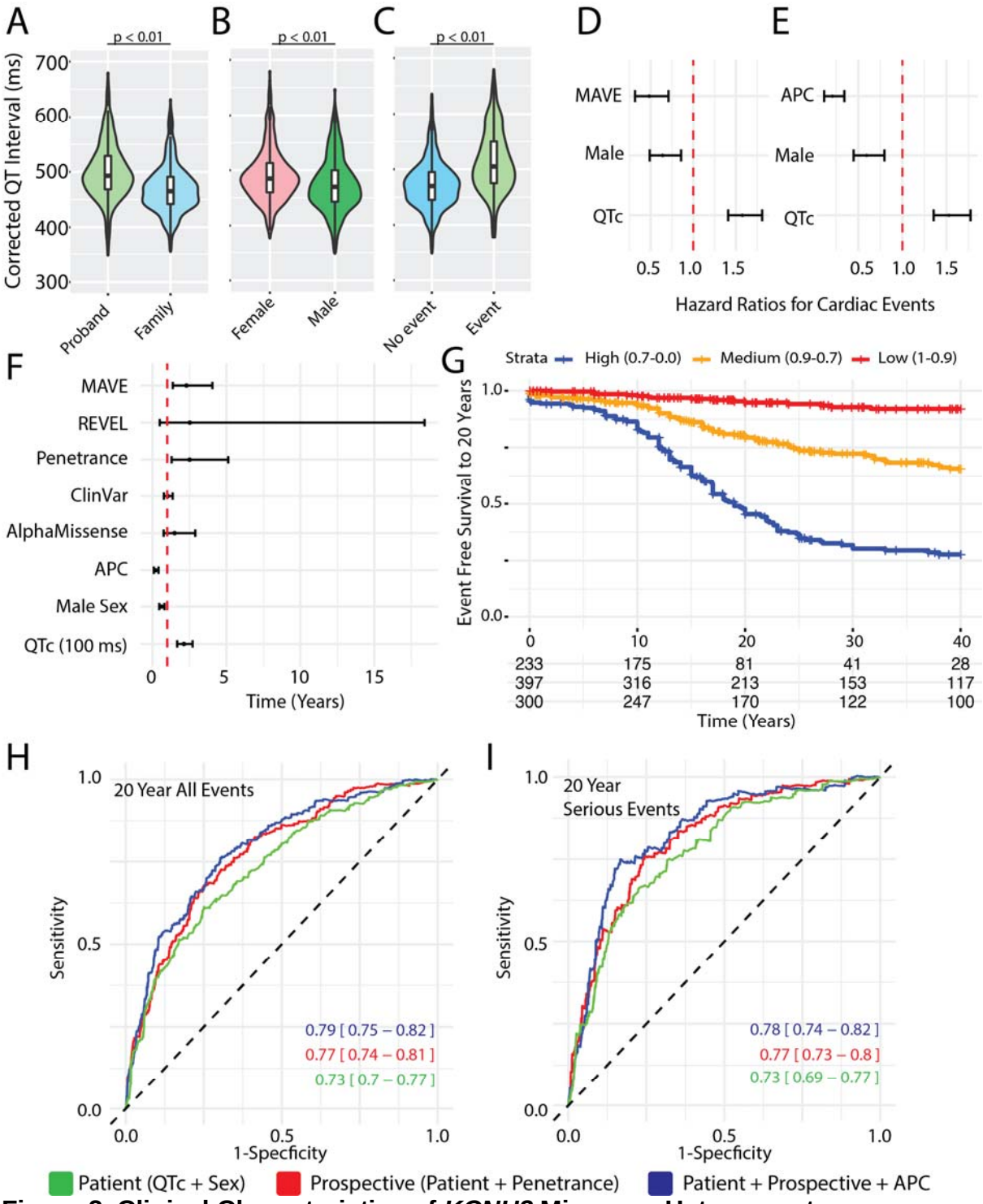

Figure 2. Clinical Characteristics of *KCNH2* Missense Heterozygotes.

A-C) Distribution of QTc among **A)** probands and families, **B)** females and males, **C)** events and no events (all $p < 0.01$; two-sided t-test).

D-E) Hazard ratios for first cardiac event with boot strapped confidence intervals using patient-specific (QTc and sex) features and **D)** MAVE functional data and **E)** APC functional data.

F) Hazard ratios for first cardiac event with model of additional variant-specific (MAVE + APC, *in silico*, ClinVar, and structural data) and patient-specific (QTc, sex) features using Royston-Parmar model.
G) Risk stratification of cardiac events at or before 40 using prospectively available tools (930 patients, 333 with at least one event).
H-I) ROCs/AUCs for three models with different covariates for all cardiac events and serious cardiac events, respectively, through 20 years of age.

Literature Cited

1 Schwartz, P. J. & Ackerman, M. J. The long QT syndrome: a transatlantic clinical approach to diagnosis and therapy. *Eur Heart J* **34**, 3109-3116 (2013). https://doi.org/10.1093/eurheartj/eht089

2 Adler, A. *et al.* An International, Multicentered, Evidence-Based Reappraisal of Genes Reported to Cause Congenital Long QT Syndrome. *Circulation* **141**, 418-428 (2020). https://doi.org/10.1161/circulationaha.119.043132

3 Richards, S. *et al.* Standards and guidelines for the interpretation of sequence variants: a joint consensus recommendation of the American College of Medical Genetics and Genomics and the Association for Molecular Pathology. *Genet Med* **17**, 405-424 (2015). https://doi.org/10.1038/gim.2015.30

4 Starita, L. M. *et al.* Variant Interpretation: Functional Assays to the Rescue. *Am J Hum Genet* **101**, 315-325 (2017). https://doi.org/10.1016/j.ajhg.2017.07.014

5 Ng, C. A. *et al.* A massively parallel assay accurately discriminates between functionally normal and abnormal variants in a hotspot domain of KCNH2. *Am J Hum Genet* (2022). https://doi.org/10.1016/j.ajhg.2022.05.003

6 Kozek, K. A. *et al.* High-throughput discovery of trafficking-deficient variants in the cardiac potassium channel K(V)11.1. *Heart Rhythm* **17**, 2180-2189 (2020). https://doi.org/10.1016/j.hrthm.2020.05.041

7 Jiang, C. *et al.* A calibrated functional patch-clamp assay to enhance clinical variant interpretation in KCNH2-related long QT syndrome. *Am J Hum Genet* **109**, 1199-1207 (2022). https://doi.org/10.1016/j.ajhg.2022.05.002

8 Floyd, B. J. *et al.* Proactive Variant Effect Mapping Aids Diagnosis in Pediatric Cardiac Arrest. *Circ Genom Precis Med* **16**, e003792 (2023). https://doi.org/10.1161/circgen.122.003792

9 Matreyek, K. A. *et al.* Multiplex assessment of protein variant abundance by massively parallel sequencing. *Nat Genet* **50**, 874-882 (2018). https://doi.org/10.1038/s41588-018-0122-z

10 Anderson, C. L. *et al.* Large-scale mutational analysis of Kv11.1 reveals molecular insights into type 2 long QT syndrome. *Nat Commun* **5**, 5535 (2014). https://doi.org/10.1038/ncomms6535

11 Karczewski, K. J. *et al.* The mutational constraint spectrum quantified from variation in 141,456 humans. *Nature* **581**, 434-443 (2020). https://doi.org/10.1038/s41586-020-2308-7

12 Thomson, K. L. *et al.* Clinical interpretation of KCNH2 variants using a robust PS3/BS3 functional patch clamp assay. *HGG Adv*, 100270 (2024). https://doi.org/10.1016/j.xhgg.2024.100270

13 Brnich, S. E. *et al.* Recommendations for application of the functional evidence PS3/BS3 criterion using the ACMG/AMP sequence variant interpretation framework. *Genome Med* **12**, 3 (2019). https://doi.org/10.1186/s13073-019-0690-2

14 Schwartz, P. J., Moss, A. J., Vincent, G. M. & Crampton, R. S. Diagnostic criteria for the long QT syndrome. An update. *Circulation* **88**, 782-784 (1993). https://doi.org/10.1161/01.cir.88.2.782

15 Rohatgi, R. K. *et al.* Contemporary Outcomes in Patients With Long QT Syndrome. *J Am Coll Cardiol* **70**, 453-462 (2017). https://doi.org/10.1016/j.jacc.2017.05.046

16 O'Neill, M. J. *et al.* Continuous Bayesian Variant Interpretation Accounts for Incomplete Penetrance among Mendelian Cardiac Channelopathies. *Genet Med* (2022). https://doi.org/10.1016/j.gim.2022.12.002

17 Kozek, K. *et al.* Estimating the Post-Test Probability of Long QT Syndrome Diagnosis for Rare KCNH2 Variants. *Circ Genom Precis Med* (2021). https://doi.org/10.1161/circgen.120.003289

18 Kroncke, B. M. *et al.* A Bayesian method to estimate variant-induced disease penetrance. *PLoS Genet* **16**, e1008862 (2020). https://doi.org/10.1371/journal.pgen.1008862

19 Aizawa, T. *et al.* Non-missense variants of KCNH2 show better outcomes in type 2 long QT syndrome. *Europace* **25**, 1491-1499 (2023). https://doi.org/10.1093/europace/euac269

20 Locati, E. H. *et al.* Age- and sex-related differences in clinical manifestations in patients with congenital long-QT syndrome: findings from the International LQTS Registry. *Circulation* **97**, 2237-2244 (1998). https://doi.org/10.1161/01.cir.97.22.2237